J. Iron Steel Res. Int. (2022) 29:1041–1051
https://doi.org/10.1007/s42243-022-00806-3

REVIEW

Recent progress in synthesis of composite powders and their applications in low-carbon refractories

Ji-yuan Luo[1] · Xin-ming Ren[2] · Xiao-chuan Chong[1] · Dong-hai Ding[1] · Bei-yue Ma[2] · Guo-qing Xiao[1] · Jing-kun Yu[2]

Received: 19 February 2022 / Revised: 14 April 2022 / Accepted: 17 April 2022 / Published online: 21 June 2022

Abstract
The development of low-carbon refractories is of great significance, but it is limited by the deteriorated properties that resulted from the decreased graphite content. Incorporating composite powders has proved to be effective in improving the properties of low-carbon refractories. The recent progress in the synthesis of composite powders including modified graphite, nanocarbon-containing composite powders, oxide/non-oxide and non-oxide composite powders and their applications in low-carbon refractories were reviewed, and the future development of composite powder technology was prospected.

Keywords Composite powder · Modified graphite · Nanocarbon-containing composite powder · Oxide/non-oxide · Non-oxide · Low-carbon refractory

1 Introduction

Carbon containing refractories are indispensable in the metallurgy process of iron and steel owing to their remarkable thermal shock resistance and slag resistance [1–4]. Among them, carbon bonded magnesia (MgO–C) [5–7] and carbon-bonded alumina (Al_2O_3–C) refractories [8–10] are currently widely used. MgO–C refractories are typically used as the lining materials of converters and electric arc furnaces as well as the slag lines of steel ladles [11–14], while Al_2O_3–C refractories are dominantly used to fabricate continuous casting components, such as slide plates, submerged entry nozzles, long nozzles, and monobloc stoppers [15–17]. Graphite serves usually as the main carbon source in carbon containing refractories. The superior performances of carbon containing refractories are mainly benefited from the unique properties of graphite including low thermal expansion coefficient, high thermal conductivity, and poor wettability and low permeability to molten steel and slags [18–20].

However, high carbon content (about 8–20 wt.%) in traditional carbon containing refractories is prone to increase the carbon pick-up in molten steel, which is not conducive for the production of clean steel. In addition, fuel consumption per ton steel increases because the heat loss is increased owing to the high thermal conductivity of graphite, which can also lead to the deformation of ladle shells. The sensitivity of graphite to oxidation leaves pores in refractory bodies accelerating the corrosion of slag as well as releasing CO_x greenhouse gases [21]. Hence, to meet the higher requirement of steel plants to refractories and save expensive natural graphite sources, it is imperative to develop low-carbon (typically less than 8 wt.%) or ultra-low-carbon (typically less than 3 wt.%) refractories [22–24]. However, directly decreasing the graphite usage usually triggers the deterioration of thermal shock resistance and slag resistance of carbon containing refractories [25, 26]. Hence, much effort has been put in improving the properties of low-carbon refractories.

Ji-yuan Luo and Xin-ming Ren contributed equally to this work.

✉ Dong-hai Ding
dingdongxauat@163.com

✉ Bei-yue Ma
maceramic@126.com

[1] College of Materials Science and Engineering, Xi'an University of Architecture and Technology, Xi'an 710055, Shaanxi, China

[2] School of Metallurgy, Northeastern University, Shenyang 110819, Liaoning, China

The heterogeneity and complexity of refractory matrix are the main factors affecting the performances of refractories. Composite powders integrate the advantages of single component and have lower preparation cost compared to most pure powders [27, 28]. A large number of studies have proved that modifying refractory matrix by composite powders is an effective way to improve the properties of refractories [29–31].

The characteristics of composite powders, such as particle size and distribution, morphology, and bonding of single element, which are crucial for their function and stability when being used in refractories, are greatly affected by the synthesis process. Besides, the synthesis cost of composite powders should be further decreased for its wide application in refractories. Therefore, preparing composite powders with good characteristics by simple and cost-effective method has also been a hot research area in recent years. Based on the characteristics of components, composite powders can be mainly classified into carbon containing composite powders, oxide/non-oxide composite powders and non-oxide composite powders. Among them, carbon containing composite powders can be further classified into modified graphite and nanocarbon containing composite powders. This paper systematically reviewed the status of the synthesis of these composite powders and their applications in low-carbon refractories.

2 Synthesis of carbon containing composite powders and their applications

2.1 Graphite modifying

The vulnerability of graphite to oxidation at high temperatures as well as its poor dispersibility further deteriorates the performances of low-carbon refractories [32, 33]. Modifying graphite with ceramic phases is a useful way to improve its oxidation resistance and service stability in low-carbon refractories [34]. Carbides, especially SiC, have been widely used in carbon containing refractories serving as raw materials or additives [35–37]. Research works on synthesizing carbides-coated graphite have been reported in recent years, which has proved to be an effective method to improve the oxidation resistance of graphite [38]. Liao et al. [39] employed silane coupling agent (SCA) as coating precursors and prepared SiC-coated expandable graphite. The complexation of SCA with dangling bonds of –OH on expanded graphite resulted in better covering and dispersion. The SCA coatings were pyrolyzed at elevated temperature, leading to the formation of SiC and amorphous SiC_xO_y coating on the surface of the expanded graphite. The oxidation resistance of the expanded graphite was remarkably enhanced owing to the existence of the composite coatings and the peak temperature was up to 812.1 °C. Liu et al. [40] prepared C–SiC composite powders by salt-assisted synthesis method with Si and graphite as raw materials. NaCl and NaF are adopted as the molten salt medium. The NaCl–NaF molten salt medium promoted the reaction between the reactants and stimulated the formation of new phases. In the scanning electron microscopy (SEM) images of the composite powders shown in Fig. 1a, SiC nano-whiskers with diameter of 10–50 nm can be found densely covering the surface of graphite. The oxidation resistance of the modified graphite was improved, and the activation energy of oxidation is 226.70 kJ mol^{-1}, higher than that of flake graphite (180.98 kJ mol^{-1}). Owing to a better protection on the graphite, higher oxidation resistance was realized in the low-carbon Al_2O_3–C refractories (graphite content 5 wt.%) containing the C–SiC composite powders. Additionally, owing to the reaction between the SiC cladding layer and the slag at high temperature, the viscosity of the slag was improved, resulting in superior slag resistance. Owing to lower synthesis temperature, shorter period, and high purity products with good homogeneity [41, 42], molten salt method is also used to prepare other carbides-coated graphite besides SiC. Li et al. [43, 44] prepared Cr_3C_2-coated flake graphite through molten salt method under flowing argon atmosphere with flake graphite and Cr powders as the starting materials and NaCl/NaF as the molten salt medium. When adjusting the reaction temperature to 950 °C and the Cr/C molar ratio to 1/2, a dense Cr_3C_2 coating on flake graphite is obtained as shown in Fig. 1b. The incorporation of Cr_3C_2-coated flake graphite certainly improved the oxidation resistance and slag resistance of low-carbon MgO–C refractories (graphite content 5 wt.%). Furthermore, the addition of the Cr_3C_2-coated flake graphite accelerated the transformation of Mg_2SiO_4 spherical grains to columnar particles, which improved the physical and mechanical properties of the refractory bodies. When the amount of the composite powders used in the refractories was 2 wt.%, the low-carbon MgO–C refractories show optimized cold modulus of rupture (CMOR) and cold crushing strength (CCS). Some other ceramic phase coatings have also proved to be positive in protecting graphite from rapid oxidation and are also helpful to improve the properties of low-carbon refractories. ZrC-coated graphite [45] (Fig. 1c) was also prepared by molten salt method with Zr powder and graphite as starting materials. The low-carbon Al_2O_3–C refractories (graphite content 4 wt.%) containing ZrC-coated graphite exhibited optimized oxidation resistance and slag resistance thanks to the protection of ZrC to graphite.

Chandra and Sarkar [46, 47] fabricated YAG ($Y_3Al_5O_{12}$) hybridized expandable graphite (EG) by mechanical milling using thermally pre-expanded graphite

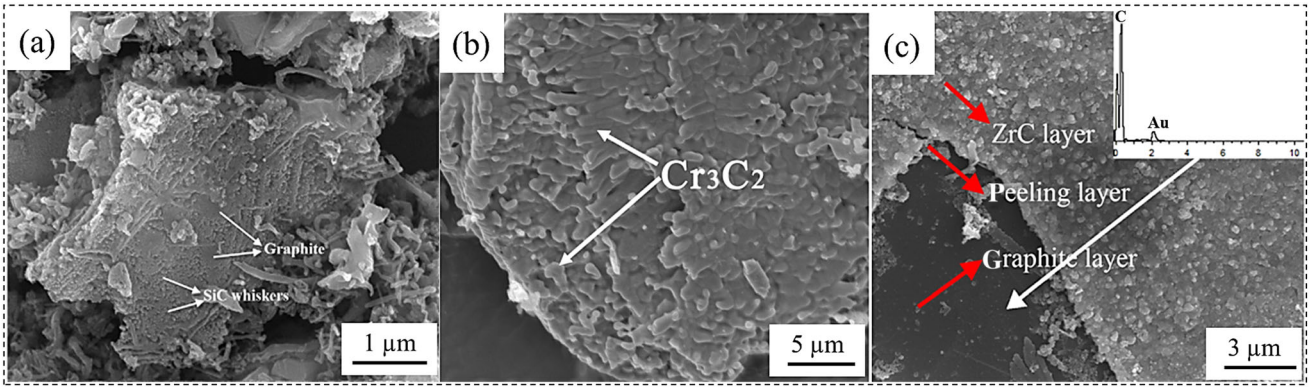

Fig. 1 Microstructures of different modified graphite. **a** SiC whiskers-coated graphite [40]; **b** Cr_3C_2-coated graphite [43]; **c** ZrC-coated graphite [45]

and YAG powders from chemical precipitation as raw materials. After mechanical milling, turbostratic disorder can be observed in the lamellar structure of the expandable graphite in the hybridized powders. The hybridized powder was then introduced into Al_2O_3–MgO–C refractories (graphite content 4 wt.%), and the compression strength, toughness, and intrinsic surface energy of the refractories were all enhanced, which can contribute to the formation of well-sintered framework of expandable graphite embedded polyhedral YAG grains in the refractory matrix, as shown in Fig. 2.

Although the modified graphite exhibits higher oxidation resistance and hence plays a positive role in improving the comprehensive properties of low-carbon refractories, the complexity and cost of the synthesis procedure, the selection of raw materials, and the stability in characteristics of the coated graphite are still key factors affecting its wide application in low-carbon refractories.

2.2 Nanocarbon containing composite powders

A series of research works have proved that substituting graphite with nanocarbons is beneficial to improve the performances of low-carbon refractories [48–53]. Owing to their small particle size, nanocarbons can effectively improve the density of refractories by filling the pores and gaps. In addition, nanocarbons, such as nanocarbon black and artificial expanded graphite, have high deformability and thus can absorb or relieve the thermal strain energy stored in refractory bodies [54–56], while carbon nanofibers, carbon nanotubes, and graphene can inhibit the propagation of microcracks through "pulling-out," "bridging," and/or "deflection" mechanisms, which are beneficial to enhance the thermal shock resistance of the refractories [57–61]. However, the high specific surface area makes nanocarbons prone to agglomerate and more sensitive to oxidation than graphite, which greatly affects

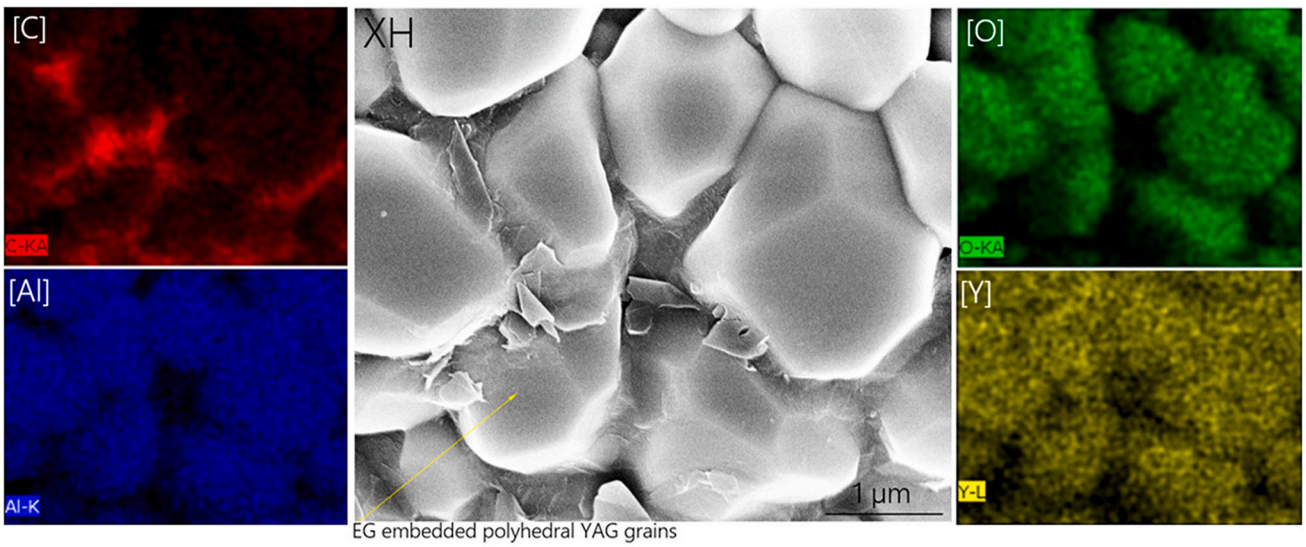

Fig. 2 Expandable graphite embedded polyhedral YAG microstructures in refractory matrix observed by SEM under high resolution [46]

the service stability of nanocarbons in refractory bodies. Additionally, high cost is also a crucial issue that inhibits the application of nanocarbons in low-carbon refractories. The poor dispersibility as well as oxidation resistance of nanocarbons can be effectively improved by synthesizing nanocarbon containing composite powders owing to the interlocking structure formed between nanocarbons and other components. The cost of nanocarbon can also be lowered in this way, and the components in the composite powders except nanocarbons can also play a positive role in improving the performance of low-carbon refractories. The characteristics of the synthesized nanocarbon containing composite powders are greatly affected by synthesis method and raw materials.

Simple and cost-effective synthesis of nanocarbon containing composite powders is one of the important factors affecting its industrial application, and the selection of synthesis method also has great influence on the characteristics of the composite powder products. Up to now, several different nanocomposite powder technologies have been exploited to synthesize nanocarbon containing composite powders including combustion synthesis and chemical vapor deposition (CVD), and satisfactory results were obtained.

Combustion synthesis, also known as self-propagating high-temperature synthesis (SHS), is a fast and simple method to prepare powder materials [62–65]. The energy consumption of this method is very low because the propagation of the combustion wave is sustained by the heat released by the reaction itself [66–68]. Ding et al. [69] prepared $B_4C/Al_2O_3/C$ nanocomposite powders by combustion synthesis with B_2O_3, carbon black, and Al powders as raw materials. The B_4C particles in the synthesized composite powders have good crystallinity and small grain sizes since there was no time for the B_4C grains to grow up during the rapid synthesis process. In addition, the B_4C particles were evenly embedded in the Al_2O_3 matrix, and the residual nanocarbon black were uniformly distributed in the powders. Owing to the unique microstructures of the composite powders, the contact between the uniformly distributed carbon black and oxygen was isolated by the B_4C particles, which improved the oxidation resistance of low-carbon MgO–C refractories (graphite content 3 wt.%). Furthermore, the agglomerate structures of the composite powders and the uniform dispersion of nanocarbon black resulted in more thermal strain energy consumption and consequently improved the thermal shock resistance of the low-carbon MgO–C refractories (Fig. 3).

CNTs/MgO composite powders [70] were also prepared by a one-step catalytic combustion synthesis method using magnesium oxalate (MgC_2O_4) as the carbon source, magnesium powders as the reductant, and nickel nitrate hexahydrate ($Ni(NO_3)_2{\cdot}6H_2O$) as the catalyst. The CNTs in the composite powders exhibit hollow bamboo-like structures with high aspect ratio, and the growth mechanism follows the V–L–S mechanism. The synthesized composite powders were then added into low-carbon Al_2O_3–C refractories (graphite content 2 wt.%). The thermal shock resistance of the refractories containing 2.5 wt.% CNTs/MgO composite powders was enhanced remarkably. The residual strength ratio of the refractory samples after three cycles of thermal shock test increased 63.9% compared to that of the reference batch.

Although the composite powders synthesized by combustion synthesis show positive effects on improving the properties of low-carbon refractories, the rapid and violent synthesis process increases the inhomogeneity of the powder products, which may affect the service stability of composite powders in refractories.

Chemical vapor deposition is a common method to prepare film or membrane materials for its high controllability and good designability of the products [71–74]. Recently, CVD method was also used to synthesize nanocarbon containing composite powders for its convenience in realizing the uniform distribution of nanocarbons as well as the high controllability in morphologies. Liang et al. [75] synthesized Al_2O_3/multi-walled carbon nanotube (MWCNT) composite powders by catalytic decomposition of methane with Fe–Ni/Al_2O_3 as the catalysts. In the composite powders, MWCNTs with diameters of about 10–50 nm were deposited on the catalyst and evenly dispersed on the surface of Al_2O_3 particles. The obtained composite powders and commercial MWCNTs were added to Al_2O_3–C refractories as CNTs sources, respectively. By comparison, the incorporation of the Al_2O_3/MWCNTs composite powders substantially improved the dispersibility of MWCNTs in the matrix, which better filled the interior pores and gaps and achieved higher densification, fracture properties, thermal shock resistance, and slag corrosion resistance of the refractory samples. In addition, superior properties were obtained owing to the in situ formation of SiC whiskers from the reaction between the MWCNTs on the surface of Al_2O_3 grains and the antioxidants Si. Moreover, the advantages of CVD method make it have great potential to modify the interface between oxides and matrix in low-carbon refractories, which have considerable effects on the thermal shock resistance of the low-carbon Al_2O_3–C refractories (graphite content 3 wt.%) owing to interface debonding effects and energy dissipation mechanisms.

Li et al. [76] synthesized nanocarbons decorated Al_2O_3 powders through CVD method adopting ethanol as the carbon source. The content of the catalyst $Ni(NO_3)_2{\cdot}6H_2O$ affects the morphologies of the nanocarbons: less catalyst led to the formation of MWCNTs, while higher content of catalyst is more conducive to the formation of nano-onion-

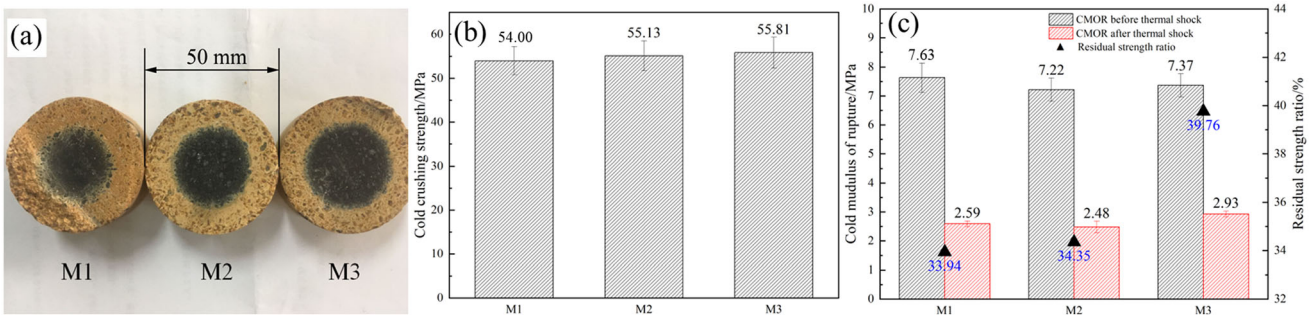

Fig. 3 Optimized performance of low-carbon MgO–C refractories with combustion synthesized $B_4C/Al_2O_3/C$ composite powders. **a** Oxidation resistance; **b** CCS; **c** CMOR and thermal shock resistance [69]

like carbon because of the agglomeration of the catalyst. The high content of MWCNTs in the composite powders stimulates the formation of SiC whiskers, which apparently improved the mechanical properties of the low-carbon Al_2O_3–C refractories (graphite content 2 wt.%). Although nano-onion-like carbon has little effects on the toughness of the refractories, the cohesion between the matrix and Al_2O_3 particles was reduced, which increased the consumption of the energy stored in the refractory bodies and hence enhanced the thermal shock resistance (Fig. 4).

Although impressive results have been obtained from the application of CVD synthesized nanocarbon containing composite powders in low-carbon refractories, there is still a long way for its wide application for the high cost as well as the high precision requirements of this method.

Besides the synthesis method, the carbon sources also significantly influence the characteristics of the morphologies and distribution of nanocarbons in the composite powder products. Contributing to the chemical bonding between metallic oxides and organic carbon, organic acids, such as magnesium oxalate, magnesium citrate, and calcium citrate, have been explored to synthesize nanocarbon containing composite powders [77–80]. Ding et al. [81] prepared multilayer graphene containing $MgAl_2O_4$ powders by sintering magnesium citrate and alumina powders in carbon embedded condition. The multilayer graphene pyrolyzed by the methane gas from the decomposition of magnesium citrate, inside or attached to the surface of the agglomerated $MgAl_2O_4$ grains. The composite powders remarkably improved the thermal shock resistance of low-carbon MgO–C (graphite content 3 wt.%) [82] and Al_2O_3–C (graphite content 2 wt.%) [83] refractories because the microcracks with many branches formed in the agglomerated structures increased the energy dissipation during thermal shock.

As mentioned above, modified graphite and nanocarbon containing composite powders can definitely improve the comprehensive performances of low-carbon refractories. The unique coating structures between the graphite/nanocarbons with other components in the composite powders and the interface between these components play a key role in improving refractory property, however, they were seldom reported. Besides, the stability in the characteristics and function of the composite powders need to be further investigated.

3 Synthesis of oxide/non-oxide composite powders and their applications

It is well known that oxides, such as Al_2O_3, ZrO_2, and MgO, have excellent resistance to extreme environment, molten steel, and slags, while non-oxide ceramic phases, such as AlB_2, ZrB_2, and SiC, play a more prominent role in

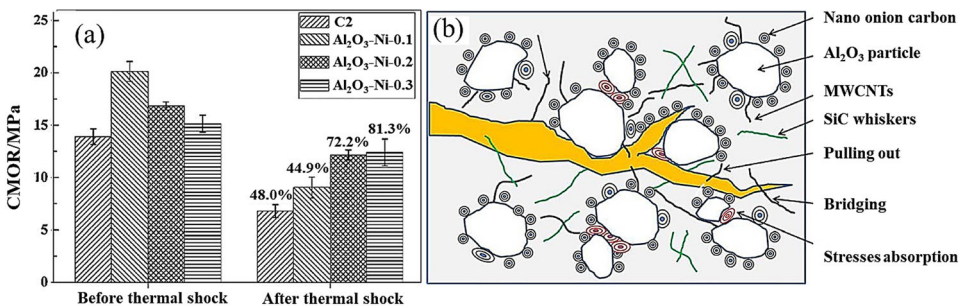

Fig. 4 Thermal shock resistance of low-carbon Al_2O_3–C refractories containing different contents of nanocarbons decorated Al_2O_3 composite powders and schematic diagram of effects of powders on propagation behavior of microcracks [76]

improving the oxidation resistance and the thermal–mechanical properties of carbon containing refractories. Hence, introducing composite powders composed of oxides and non-oxides can integrate the advantages of these two components and have a synergistic effect on improving the service performances of low-carbon refractories. AlB_2 is an ideal antioxidant protecting graphite from oxidation at middle temperatures of about 400–1000 °C. However, the complexity and high cost of synthesizing pure AlB_2 powders limit its wide application. To solve this problem, AlB_2–Al–Al_2O_3 [84, 85] composite powders were prepared by combustion synthesis with Al powders and B_2O_3 as raw materials. The microstructural evolution during the process followed a dissolution–precipitation mechanism. The AlB_2–Al–Al_2O_3 composite powders [86] were then introduced into low-carbon MgO–C refractories (graphite content 3 wt.%) as antioxidants, and their effects on the oxidation resistance of the refractories were compared with that of the conventional antioxidants Al/Si and Al powders. The results showed that the oxidation product of the composite powders was $Mg_3B_2O_6$, which melted at 1400 °C and consequently better filled the pores and blocked the gas channels in the matrix. Hence, the composite powder was superior to Al/Si and Al powders as antioxidant used in the low-carbon MgO–C refractories.

Although substituting pure powders with composite powders obtained satisfactory results meanwhile lowering the production cost, the use of high-purity chemical raw materials makes the cost of the composite powders still high. Employing cheap minerals and even some industrial solid wastes as raw materials to prepare composite powders is of great potential to further reduce the cost of composite powders and accelerate its wide application. Based on this concept, Ma et al. synthesized Al_2O_3–SiC composite powders from pyrophyllite [87], coal ash [88], electroceramics waste [89], and clay [90], respectively. Figure 5 presents the SEM images of these Al_2O_3–SiC composite powders synthesized from different raw materials, and they are similar in size, all in the micron scale. Furthermore, as an applicability exploration, the above Al_2O_3–SiC composite powders were introduced into low-carbon MgO–C refractories (graphite content 4 wt.%), and the effects on the oxidation resistance and slag resistance were mainly investigated. As shown in Fig. 6, the oxidation resistance and slag resistance of the low-carbon MgO–C samples are improved to a certain extent. The authors attribute this beneficial effect to the in situ formation of spinel and forsterite. Specifically, the volume expansion effect accompanying the formation of spinel and forsterite effectively filled the pores and gaps of the low-carbon MgO–C sample; in addition, key properties such as melting point and viscosity of the slag are changed, thereby delaying further corrosion of the slag. Furthermore, there are some easy-to-prepare and low-cost composite powders that deserve more attention, such as ZrB_2–SiC (from zircon and boron oxide) [91], ZrN–SiAlON (from zircon and bauxite) [92], and SiC–SiAlON (from kyanite tailings) [93].

4 Synthesis of non-oxide composite powders and their applications

The combination of different non-oxides, including ZrB_2, SiC, ZrN, etc., can also achieve optimized properties of refractories compared to pure powders. Huang et al. [94] pre-synthesized Sialon–ZrN composite powders by carbothermal reduction method with inexpensive low-grade bauxite and zirconite as raw materials and introduced the composite powders into SiC particles to fabricate free-fired refractories. The resistance of the SiC-based free-fired refractories to blast furnace slag was improved because the ZrO_2 from the oxidation of ZrN formed protective phases with low melting point. ZrB_2–SiCw (w-whisker) composite powders were successfully synthesized by Ban et al. [95] through microwave-assisted carbo/borothermal reduction method under the protection of argon gas with zircon, boric acid and activated carbon as raw materials. The composite powders exhibited low thermal expansion, good oxidation resistance and poor wettability against slags, and these

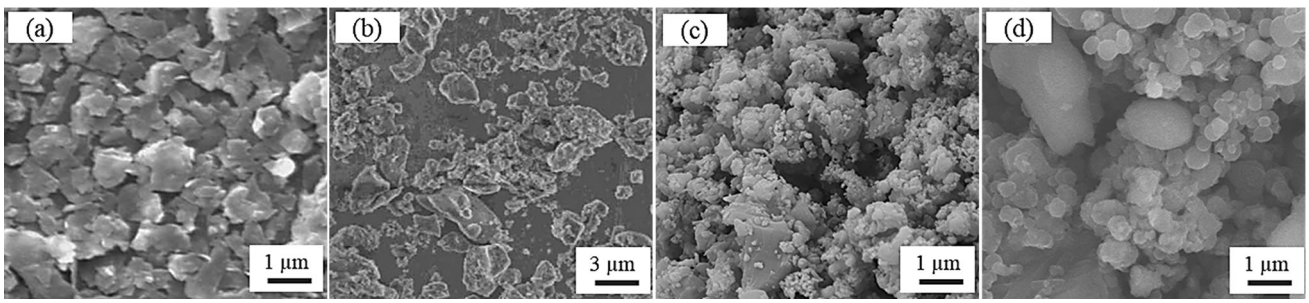

Fig. 5 SEM images of Al_2O_3–SiC composite powders synthesized from pyrophyllite (1700 °C for 4 h) [87], coal ash (1550 °C for 5 h) [88], electroceramics waste (1600 °C for 4 h) [89], and clay (600 A for 15 min) [90]

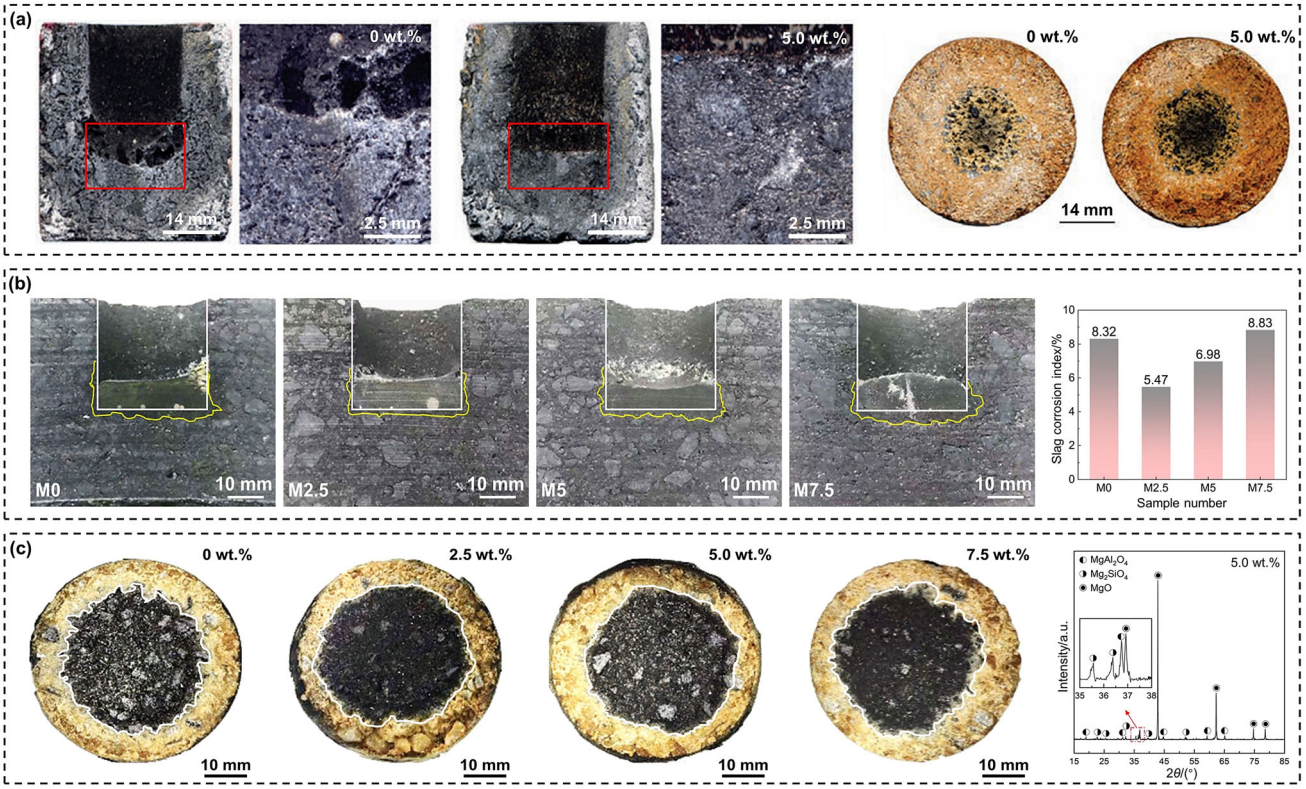

Fig. 6 Oxidation resistance and slag resistance of low-carbon MgO–C samples with Al_2O_3–SiC composite powders synthesized from pyrophyllite (**a**, 5.0 wt.%) [87], electroceramics waste (**b**, 0–7.5 wt.%) [89], and clay (**c** 0–7.5 wt.%) [90]

characteristics resulted in higher thermal–mechanical properties and corrosion resistance of the Al_2O_3–ZrO_2–C refractories (graphite content 2 wt.%) with adding the ZrB_2–SiCw composite powders. In addition, some other non-oxide composite powders with remarkable characteristics, such as $Al_4Si_2C_5$ powders [96] and ZrB_2–SiC composite powders [97], were also prepared by researchers while the study of their effects on the properties of refractories is still in progress.

Table 1 gives a summary of the synthesis methods of different composite powders and their effects on the properties of low-carbon refractories.

5 Conclusions

Contemporary research works have proved that the introduction of composite powders including modified graphite, nanocarbon containing composite powders, oxide/non-oxide and non-oxide composite powders shows positive effects on the properties of low-carbon refractories. The insulation from ceramic coatings effectively improves the oxidation resistance of modified graphite and hence improves its service stability at high temperatures in low-carbon refractories. The addition of nanocarbon containing composite powders achieves a more uniform distribution of nanocarbons in refractories and consequently results in superior comprehensive performances. The potential of oxide/non-oxide and non-oxide composite powders is further exploited since they can be prepared from cheap minerals and industrial wastes.

One-step synthesis of composite powders could be the mainstream in the future. Furthermore, it is of great importance to clarify the relations among synthesis process, interactions between each component, characteristics and properties of composite powders, their effects on refractory properties and the function mechanisms. The interface between each component greatly affects the properties of composite powders; however, relevant research works were seldom reported. Besides, the stability of nanocomposite powders at high temperatures in long-time service cycles in refractories needs to be further discussed.

Table 1 Summary of synthesis of composite powders and their effects on properties of low-carbon refractories

Classification	Composite powders	Raw materials	Synthesis method	Application (graphite content/wt.%)	Refractory property improvement	Mechanism
Graphite modifying	C–SiC whiskers [40]	Si, flake graphite, NaCl/NaF (molten salt medium)	Molten salt method	Al_2O_3–C (5)	Oxidation resistance, slag resistance, CMOR	SiC prevents graphite from rapid oxidation; SiC layers reacting with slag increase its viscosity
	Cr_3C_2-coated flake graphite [43]	Cr, C, NaCl/NaF (molten salt medium)	Molten salt method	MgO–C (5)	Bulk density, apparent porosity, CMOR, CCS, pore diameter	Formation of columnar Mg_2SiO_4
	ZrC-coated graphite [45]	Zr, graphite	Molten salt method	Al_2O_3–C (4)	Oxidation resistance, slag resistance	ZrC protects graphite from rapid oxidation
	Nano-YAG hybridized expandable graphite [46]	YAG, EG	Mechanical milling	Al_2O_3–MgO–C (4)	Compression strength, toughness, intrinsic surface energy, Weibull modulus, thermal shock resistance (↑166.6%)	Well-sintered frame work of expandable graphite embedded polyhedral YAG grains throughout matrix
Nanocarbon containing	$B_4C/Al_2O_3/C$ [69]	B_2O_3, carbon black, Al	Combustion synthesis	MgO–C (3)	Bulk density, apparent porosity, oxidation resistance, slag resistance, thermal shock resistance (↑17.2%)	More uniform B_4C better protects carbon black; uniform carbon black consumes more strain energy
	CNTs/MgO [70]	Magnesium oxalate, Mg, $Ni(NO_3)_2{\cdot}6H_2O$	Catalytic combustion synthesis	Al_2O_3–C (2)	Thermal shock resistance (↑63.9%)	Toughening effects of MWCNTS
	Al_2O_3/MWCNTs [75]	Al_2O_3, $Fe(NO_3)_3{\cdot}9H_2O$, $Ni(NO_3)_2{\cdot}6H_2O$, methane	Catalytic deposition	Al_2O_3–C (3)	Densification, fracture properties, slag resistance, thermal shock resistance (↑105.4%)	"Bridging" and "pulling out" of uniformly distributed MWCNTS
	MWCNTs/nano-onion-like carbon decorated Al_2O_3 [76]	Reactive alumina, ethanol, $Ni(NO_3)_2{\cdot}6H_2O$	CVD	Al_2O_3–C (2)	CMOR, elastic modulus, thermal shock resistance (↑69.4%)	"Bridging" and "pulling out" of MWCNTS, formation of SiC whiskers; reduced cohesion of matrix and Al_2O_3 particles
	Multilayer graphene containing $MgAl_2O_4$ [82, 83]	Magnesium citrate, Al_2O_3	Protective sintering	Al_2O_3–C (2) MgO–C (3)	Oxidation resistance, slag resistance, thermal shock resistance (↑80%, ↑57.1%)	Formation of microcracks with many branches and fibrous ceramic phases; $MgAl_2O_4$ increased slag viscosity

Table 1 (continued)

Classification	Composite powders	Raw materials	Synthesis method	Application (graphite content/ wt.%)	Refractory property improvement	Mechanism
Oxide/non-oxide integrate	ZrO_2–SiC [98]	Zircon, carbon black	Carbothermal reduction	Al_2O_3–C (15)	Bulk density, crushing strength, thermal shock resistance (↑702%)	Phase transformation of ZrO_2
	AlB_2–Al–Al_2O_3 [86]	Al, B_2O_3	Combustion synthesis	MgO–C (3)	Oxidation resistance	$Mg_3B_2O_6$ formed and melted at 1400 °C, filling pores and blocking gas channels
	Al_2O_3–SiC [87]	Pyrophyllite, natural graphite	Carbothermal reduction	MgO–C (4)	Slag resistance	Increase in slag viscosity and formation of $MgAl_2O_4$
	Al_2O_3–SiC [89]	Electroceramics waste, carbon black	Carbothermal reduction	MgO–C (4)	CCS, thermal shock resistance (↑17.18%), oxidation resistance, slag resistance	Formation of spinel- and forsterite-containing dense protective layer
	Al_2O_3–SiC [90]	Clay, carbon black	Electromagnetic induction heating	MgO–C (4)	Apparent porosity, CCS, thermal shock resistance (↑15.01%), oxidation resistance	Volume expansion caused by in situ formation of spinel and forsterite
	ZrB_2–SiCw [95]	Zircon, boric acid and activated carbon	Carbo/ borothermal reduction	Al_2O_3–ZrO_2–C (2)	Corrosion resistance, cold modulus of rupture, hot modulus of rupture, thermal shock resistance (↑65%–85%)	Low expansion coefficient, good conductivity, and poor wettability to slags of ZrB_2–SiCw

Acknowledgements The authors thankfully acknowledge the financial support of the National Natural Science Foundation of China (Nos. U20A20239, U1908227, and 51772236) for sponsoring this work.

References

[1] E.M.M. Ewais, J. Ceram. Soc. Jpn. 112 (2004) 517–532.
[2] X.M. Ren, B.Y. Ma, S.M. Li, H.X. Li, G.Q. Liu, S.X. Zhao, W.G. Yang, F. Qian, J.K. Yu, J. Aust. Ceram. Soc. 55 (2019) 913–920.
[3] A.P. Luz, R. Salomão, C.S. Bitencourt, C.G. Renda, A.A. Lucas, C.G. Aneziris, V.C. Pandolfelli, Open Ceram. 3 (2020) 100025.
[4] S.S. Li, J.H. Liu, J.K. Wang, Q. Zhu, X.W. Zhao, H.J. Zhang, S.W. Zhang, Int. J. Appl. Ceram. Technol. 15 (2018) 1166–1181.
[5] M. Ludwig, E. Śnieżek, I. Jastrzębska, R. Prorok, M. Sułkowski, C. Goławski, C. Fischer, K. Wojteczko, J. Szczerba, Constr. Build. Mater. 272 (2021) 121912.
[6] Y. Cheng, T.B. Zhu, Y.W. Li, S.B. Sang, Ceram. Int. 47 (2021) 2538–2546.
[7] X.M. Ren, B.Y. Ma, S.M. Li, H.X. Li, G.Q. Liu, W.G. Yang, F. Qian, S.X. Zhao, J.K. Yu, J. Iron Steel Res. Int. 28 (2021) 38–45.
[8] X.W. Wei, A. Yehorov, E. Storti, S. Dudczig, O. Fabrichnaya, C.G. Aneziris, O. Volkova, Adv. Eng. Mater. 24 (2022) 2100718.
[9] C. Atzenhofer, S. Gschiel, H. Harmuth, J. Eur. Ceram. Soc. 37 (2017) 1805–1810.
[10] J.F. Chen, L.G. Chen, Y.W. Wei, N. Li, S.W. Zhang, Corros. Sci. 143 (2018) 166–176.
[11] Q. Gu, G.Q. Liu, H.X. Li, Q.L. Jia, F. Zhao, X.H. Liu, Ceram. Int. 45 (2019) 24768–24776.
[12] J.F. Chen, N. Li, J. Hubálková, C.G. Aneziris, J. Eur. Ceram. Soc. 38 (2018) 3387–3394.
[13] R. Sarkar, B.P. Nash, H.Y. Sohn, J. Eur. Ceram. Soc. 40 (2020) 529–531.
[14] Q. Gu, T. Ma, F. Zhao, Q.L. Jia, X.H. Liu, G.Q. Liu, H.X. Li, J. Alloy. Compd. 847 (2020) 156339.
[15] J. Zhang, X.C. Li, W. Gong, P.A. Chen, B.Q. Zhu, J. Eur. Ceram. Soc. 39 (2019) 2739–2747.
[16] Z. Chen, W. Yan, S. Schafföner, Y.W. Li, N. Li, J. Alloy. Compd. 862 (2021) 158036.

[17] C.F. Yin, X.C. Li, P.A. Chen, B.Q. Zhu, Ceram. Int. 45 (2019) 7427–7436.
[18] M.Q. Liu, J.T. Huang, Q.M. Xiong, S.Q. Wang. Z. Chen, X.B. Li, Q.W. Liu, S.W. Zhang, Nanomaterials 9 (2019) 1242.
[19] X.L. Shang, X.Y. Tian, H.X. Li, X.F. Wang, G.Q. Liu, W.G. Yang, J. Chin. Ceram. Soc. 47 (2019) 412–418.
[20] S.S. Li, J.H. Liu, J.K. Wang, L. Han, H.J. Zhang, S.W. Zhang, Ceram. Int. 44 (2018) 12940–12947.
[21] J.T. Huang, M.Q. Liu, Z.H. Sun, X.L. Hou, X.B. Li, Z. Chen, Z.H. Hu, J.T. Ma, Z.J. Feng, Rare Metal Mater. Eng. 49 (2020) 682–687.
[22] X.M. Ren, B.Y. Ma, H. Liu, Z.F. Wang, C.J. Deng, G.Q. Liu, J.K. Yu, J. Eur. Ceram. Soc. 42 (2022) 3986–3995.
[23] T.B. Zhu, Y.W. Li, S.B. Sang, S.L. Jin, J. Ceram. Sci. Technol. 7 (2016) 127–134.
[24] G.F. Liu, N. Liao, M. Nath, Y.W. Li, S.B. Sang, J. Eur. Ceram. Soc. 41 (2021) 2948–2957.
[25] Y. Chen, C.J. Deng, X. Wang, C. Yu, J. Ding, H.X. Zhu, J. Eur. Ceram. Soc. 41 (2021) 963–977.
[26] Z. Gao, B.Y. Ma, J. Iron Steel Res. 33 (2021) 353–362.
[27] J.Y. Luo, G.Q. Xiao, D.H. Ding, X.C. Chong, J.C. Ren, B. Bai, Ceram. Int. 47 (2021) 29607–29619.
[28] Q.L. Chen, T.B. Zhu, Y.W. Li, Y. Cheng, N. Liao, L.P. Pan, X. Liang, Q.H. Wang, S.B. Sang, Ceram. Int. 47 (2021) 20178–20186.
[29] H. Xu, X.T. Wang, Z.F. Wang, Y. Ma, H. Liu, Y.L. Wang, J. Alloy. Compd. 766 (2018) 759–768.
[30] C. Yu, K.R. Cheng, J. Ding, C.J. Deng, Z.L. Xue, X.X. Wu, H.X. Zhu, Ceram. Int. 43 (2017) 11415–11420.
[31] H.X. Li, J.K. Yu, K. Hiragushi, China's Refract. 9 (2000) No.2, 3–6.
[32] M. Raju, S.C. K, T. Mahata, D. Sarkar, H.S. Maiti, J. Eur. Ceram. Soc. 42 (2022) 1804–1814.
[33] X.F. Xu, T.B. Zhu, Y.W. Li, Y.J. Dai, M. Nath, Y.C. Ye, N.Y. Hu, Y.J. Li, X.Y. Wang, J. Eur. Ceram. Soc. 42 (2022) 672–681.
[34] X. Xu, Y. Li, Q. Wang, S. Sang, L. Pan, J. Ceram. Sci. Technol. 8 (2017) 455–462.
[35] C. Atzenhofer, H. Harmuth, J. Eur. Ceram. Soc. 41 (2021) 7330–7338.
[36] J.L. Xiao, J.F. Chen, Y.W. Wei, Y. Zhang, S.W. Zhang, N. Li, Ceram. Int. 45 (2019) 21099–21107.
[37] Y. Zhang, J.F. Chen, N. Li, Y.W. Wei, B.Q. Han, Y.P. Cao, G.Q. Li, Ceram. Int. 44 (2018) 16435–16442.
[38] J.K. Ye, S.W. Zhang, W.E. Lee, J. Eur. Ceram. Soc. 33 (2013) 2023–2029.
[39] N. Liao, Y.W. Li, J.B. Shan, T.B. Zhu, S.B. Sang, D.C. Jia, Ceram. Int. 44 (2018) 3319–3325.
[40] Z.L. Liu, C.J. Deng, C. Yu, X. Wang, J. Ding, H.X. Zhu, Ceram. Int. 44 (2018) 13944–13950.
[41] J.H. Liu, Z. Huang, C.G. Huo, F.L. Li, H.J. Zhang, S.W. Zhang, J. Am. Ceram. Soc. 99 (2016) 2895–2898.
[42] Z.T. Liu, J.K. Xu, X.Q. Xi, J. Zhou, J. Eur. Ceram. Soc. 42 (2022) 1302–1310.
[43] W. Li, X. Wang, C.J. Deng, C. Yu, J. Ding, H.X. Zhu, Adv. Powder Technol. 32 (2021) 2566–2576.
[44] W. Li, C.J. Deng, C. Yang, X. Wang, C. Yu, Z. Ding, H.X. Zhu, Ceram. Int. 48 (2022) 15227–15235.
[45] X. Wang, Y. Chen, C. Yu, J. Ding, D. Guo, C.J. Deng, H.X. Zhu, J. Alloy. Compd. 788 (2019) 739–747.
[46] K.S. Chandra, D. Sarkar, J. Eur. Ceram. Soc. 41 (2021) 3782–3797.
[47] K.S. Chandra, D. Sarkar, Mater. Sci. Eng. A 803 (2021) 140502.
[48] T.B. Zhu, Y.W. Li, S.B. Sang, Z.P. Xie, Ceram. Int. 42 (2016) 18833–18843.
[49] T.B. Zhu, Y.W. Li, S.B. Sang, S.L. Jin, Y.B. Li, L. Zhao, X. Liang, Ceram. Int. 40 (2014) 4333–4340.
[50] M. Bag, S. Adak, R. Sarkar, Ceram. Int. 38 (2012) 2339–2346.
[51] M. Bag, S. Adak, R. Sarkar, Ceram. Int. 38 (2012) 4909–4914.
[52] V. Pilli, R. Sarkar, J. Alloy. Compd. 781 (2019) 149–158.
[53] V. Roungos, C.G. Aneziris, Ceram. Int. 38 (2012) 919–927.
[54] H.B. Fan, Y.W. Li, S.B. Sang, Mater. Sci. Eng. A 528 (2011) 3177–3185.
[55] V. Pilli, R. Sarkar, J. Alloy. Compd. 735 (2018) 1730–1736.
[56] S. Behera, R. Sarkar, Int. J. Appl. Ceram. Technol. 11 (2014) 968–976.
[57] T.B. Zhu, Y.W. Li, S.L. Jin, S.B. Sang, N. Liao, Ceram. Int. 41 (2015) 3541–3548.
[58] S. Darban, M.G. Kakroudi, M.B. Vandchali, N.P. Vafa, F. Rezaei, V. Charkhesht, Ceram. Int. 46 (2020) 20954–20962.
[59] N. Liao, Y.W. Li, S.L. Jin, S.B. Sang, H. Harmuth, J. Eur. Ceram. Soc. 36 (2016) 867–874.
[60] Q.H. Wang, Y.W. Li, M. Luo, S.B. Sang, T.B. Zhu, L. Zhao, Ceram. Int. 40 (2014) 163–172.
[61] M. Bach, P. Gehre, H. Biermann, C.G. Aneziris, Ceram. Int. 46 (2020) 12574–12583.
[62] K.C. Patil, S.T. Aruna, T. Mimani, Curr. Opin. Solid State Mater. Sci. 6 (2002) 507–512.
[63] G.H. Liu, K.X. Chen, J.T. Li, Scripta Mater. 157 (2018) 167–173.
[64] B.H. Wang, M.J. Leonardi, W. Huang, Y. Chen, L. Zeng, B.J. Eckstein, T.J. Marks, A. Facchetti, Adv. Electron. Mater. 5 (2019) 1900540.
[65] M. Zahiri, M. Shafiee Afarani, A.M. Arabi, Appl. Phys. A 124 (2018) 663.
[66] I.V. Iatsyuk, Y.S. Pogozhev, E.A. Levashov, A.V. Novikov, N.A. Kochetov, D.Y. Kovalev, J. Eur. Ceram. Soc. 38 (2018) 2792–2801.
[67] N. Lu, G. He, J.X. Liu, G.H. Liu, J.T. Li, Ceram. Int. 44 (2018) 2463–2469.
[68] M. Akhlaghi, S.A. Tayebifard, E. Salahi, M. Shahedi Asl, G. Schmidt, Ceram. Int. 44 (2018) 9671–9678.
[69] D.H. Ding, X.C. Chong, G.Q. Xiao, L.H. Lv, C.K. Lei, J.Y. Luo, Y.F. Zang, Ceram. Int. 45 (2019) 16433–16441.
[70] G.D. Li, D.H. Ding, G.Q. Xiao, E.D. Jin, J.Y. Luo, C.K. Lei, Ceram. Int. 48 (2022) 10601–10612.
[71] B. Deng, Z.F. Liu, H.L. Peng, Adv. Mater. 31 (2019) 1800996.
[72] H.M. Park, J.Y. Lee, K.Y. Jee, S.I. Nakao, Y.T. Lee, Sep. Purif. Technol. 254 (2021) 117642.
[73] A. Baux, S. Jacques, A. Allemand, G.L. Vignoles, P. David, T. Piquero, M.P. Stempin, G. Chollon, J. Eur. Ceram. Soc. 41 (2021) 3274–3284.
[74] F. Ye, Q. Song, Z.C. Zhang, W. Li, S.Y. Zhang, X.W. Yin, Y.Z. Zhou, H.W. Tao, Y.S. Liu, L.F. Cheng, L.T. Zhang, H.J. Li, Adv. Funct. Mater. 28 (2018) 1707205.
[75] F. Liang, N. Li, B.K. Liu, Z.Y. He, Metall. Mater. Trans. B 47 (2016) 1661–1668.
[76] Y.W. Li, J.B. Shan, N. Liao, S.B. Sang, D.C. Jia, J. Eur. Ceram. Soc. 38 (2018) 3379–3386.
[77] L.H. Lv, G.Q. Xiao, D.H. Ding, Y. Ren, S.L. Yang, P. Yang, X. Hou, Int. J. Appl. Ceram. Technol. 16 (2019) 1253–1263.
[78] A. Huczko, M. Kurcz, A. Dąbrowska, M. Bystrzejewski, P. Strachowski, S. Dyjak, R. Bhatta, B. Pokhrel, B.P. Kafle, D. Subedi, Phys. Status Solidi B 253 (2016) 2486–2491.
[79] Y.Q. Zhu, H.T. Yi, X.Y. Chen, Z.H. Xiao, Ind. Eng. Chem. Res. 54 (2015) 4956–4964.
[80] R. Sun, C.W. Tai, M. Strømme, O. Cheung, ACS Appl. Nano Mater. 2 (2019) 778–789.
[81] D.H. Ding, L.H. Lv, G.Q. Xiao, Y. Ren, S.L. Yang, P. Yang, X. Hou, Ceram. Int. 45 (2019) 6209–6215.
[82] D.H. Ding, L.H. Lv, G.Q. Xiao, J.Y. Luo, C.K. Lei, Y. Ren, S.L. Yang, P. Yang, X. Hou, Int. J. Appl. Ceram. Technol. 17 (2020) 645–656.

[83] L.H. Lv, G.Q. Xiao, D.H. Ding, Ceram. Int. 47 (2021) 20169–20177.
[84] P. Yang, G.Q. Xiao, D.H. Ding, Y. Ren, Z.W. Zhang, S.L. Yang, W. Zhang, Refract. Ind. Ceram. 60 (2019) 46–54.
[85] P. Yang, G.Q. Xiao, D.H. Ding, Y. Ren, S.L. Yang, L.H. Lv, X. Hou, Mater. Res. Express. 5 (2018) 055029.
[86] P. Yang, G.Q. Xiao, D.H. Ding, Y. Ren, S.L. Yang, L.H. Lv, X. Hou, Y.Q. Gao, Ceram. Int. 48 (2022) 1375–1381.
[87] B.Y. Ma, Q. Zhu, Y. Sun, J.K. Yu, Y. Li, J. Mater. Sci. Technol. 26 (2010) 715–720.
[88] B.Y. Ma, X.M. Ren, Y. Yin, L. Yuan, Z. Zhang, Z.Q. Li, G.Q. Li, Q. Zhu, J.K. Yu, Ceram. Int. 43 (2017) 11830–11837.
[89] B.Y. Ma, X.M. Ren, Z. Gao, J.L. Tian, Z.H. Jiang, W.Y. Zan, J.K. Yu, F. Qian, Y.N. Cao, G.F. Fu, Int. J. Appl. Ceram. Technol. 19 (2022) 1265–1273.
[90] B.Y. Ma, X.M. Ren, Z. Gao, F. Qian, Z.Y. Liu, G.Q. Liu, J.K. Yu, G.F. Fu, J. Iron Steel Res. Int. (2021) https://doi.org/10.1007/s42243-021-00653-8.
[91] X.G. Deng, S. Du, H.J. Zhang, F.L. Li, J.K. Wang, W.G. Zhao, F. Liang, Z. Huang, S.W. Zhang, Ceram. Int. 41 (2015) 14419–14426.
[92] Z.J. Zhang, X.W. Wu, H. Zhao, J. Liu, H. Porwal, Z.H. Huang, Y.G. Liu, M.H. Fang, X. Min, Adv. Appl. Ceram. 116 (2017) 151–157.
[93] X. Min, M.H. Fang, Z.H. Huang, G.F. Jin, Y.G. Liu, C. Tang, X.W. Wu, H.X. Zhang, Z.X. Guo, JOM 67 (2015) 1379–1384.
[94] J.T. Huang, Z.H. Huang, Y.G. Liu, M.H. Fang, H.T. Liu, X.W. Cao, X.C. Li, M.Y. Yin, R.L. Wen, H. Tang, Ceram. Int. 40 (2014) 9763–9773.
[95] J.J. Ban, C.J. Zhou, L. Feng, Q.L. Jia, X.H. Liu, J.H. Hu, Ceram. Int. 46 (2020) 9817–9825.
[96] C. Yu, C.J. Deng, H.X. Zhu, Z.L. Xue, J. Ding, S.M. Zhou, Adv. Powder Technol. 28 (2017) 177–184.
[97] F.L. Li, C. Tan, J.H. Liu, J.K. Wang, Q.L. Jia, H.J. Zhang, S.W. Zhang, Ceram. Int. 45 (2019) 9611–9617.
[98] B.Y. Ma, J.K. Yu, Trans. Nonferrous Met. Soc. China 17 (2007) 996–1000.